FACTA UNIVERSITATIS
Series: **Physics, Chemistry and Technology** Vol. 21, Nº 1, 2023, pp. 27 - 37
https://doi.org/10.2298/FUPCT2301027J

Original scientific paper

LIGNAN PROFILE IN FRUITS OF WILD CHERVIL (*ANTHRISCUS SYLVESTRIS* (L.) HOFFM.)

UDC 547.9 : 582.893.6

Mina Janković[1], Sanja Berežni[2], Dejan Orčić[2]

[1]University of Novi Sad, Faculty of Medicine, Novi Sad, Serbia
[2]Department of Chemistry, Biochemistry and Environmental Protection, University of Novi Sad, Faculty of Sciences, Novi Sad, Serbia

Abstract. *Wild chervil (Anthriscus sylvestris (L.) Hoffm.), known also as cow parsley, is a widely distributed herbaceous plant from Apiaceae family. Traditional use as analgesic, antipyretic, antitussive, tonic, diuretic etc. is associated with the proven presence of various types of biomolecules, primarily lignans that possess cytotoxic, antiproliferative, insecticidal, antiviral and other activities. The majority of lignans reported in A. sylvestris belong to two classes – aryltetralins and dibenzylbutyrolactones. The data of lignan profile of A. sylvestris are mostly limited to root and herb composition, therefore LC-DAD-ESI-MS/MS analysis was used for the tentative identification of 15 compounds from the fruit extract of A. sylvestris, of which two were never reported in nature.*

Key words: *Anthriscus sylvestris, Apiaceae, ESI-MS, HPLC, lignan, structure elucidation.*

1. INTRODUCTION

Anthriscus sylvestris (L.) Hoffm., well known as wild chervil, is an Apiaceae species widely distributed in Europe, Asia and North America. That is a perennial, monocarpic, herbaceous plant (Dall'Acqua et al., 2006), considered an invasive, noxious weed (Miller and D'Auria, 2011). Traditional consumption of species *A. sylvestris* as an analgesic, antipyretic, antitussive, diuretic, antihypertensive and others (Orčić et al., 2022a), was justified by phytochemical studies that confirmed the presence of numerous types of biomolecules (Olaru et al., 2016; Orčić et al., 2022a; Chupakhina and Maslennikov, 2004; Chen et al., 2014; Milovanović et al., 1996; Orčić, 2010; Orčić et al., 2022b), primarily lignans (Orčić et al., 2021), which have been proven to possess biological

Received: November 13th, 2023; accepted: December 24th, 2023
Corresponding author: Dejan Orčić, Department of Chemistry, Biochemistry and Environmental Protection, University of Novi Sad, Faculty of Sciences, Trg Dositeja Obradovića 3, 21102, Novi Sad, Serbia, e-mail: dejan.orcic@dh.uns.ac.rs

activities such as antiproliferative, anti-inflammatory, cytotoxic, antiviral (Lin et al., 2004) and insecticidal (Kozawa et al., 1982). Certain semi-synthetic representatives of lignans, such as etoposide and teniposide, are used in official medicine as cytostatics, in cancer therapy (Hendrawati et al., 2011).

The two most abundant lignan classes present in *A. sylvetris* are aryltetralins and dibenzylbutyrolactones, which have been found in all parts of the plant. The majority of studies refers to the roots (Orčić et al., 2021; Kozawa et al., 1982) and herbs (Orčić et al., 2022a; Dall'Acqua et al., 2006), while literature data on the qualitative analysis of lignans from the fruits are still scarce and limited to confirmed presence of deoxypodophyllotoxin, morelensin, yatein and (-)-hinokinin (Ikeda et al., 1998).

In this paper, using LC-DAD-MS and LC-DAD-MS/MS methods, we performed structure elucidation by interpretation of MS^1, MS^2, UV spectra and automatic search of the internal library of lignans' mass spectra (Orčić et al., 2021).

3. MATERIALS AND METHODS

2.1. General

Chemicals – methanol and formic acid – were obtained from Merck (Darmstadt, Germany).

2.2. Plant material

Plant material was collected at June 7th 2023, from Fruška Gora mountain (45.15727°N, 19.79375°E) in north-western part of Serbia, during the senescence phase, and air-dried. The voucher specimen was confirmed and deposited at the Herbarium of the Department of Biology and Ecology (BUNS Herbarium), Faculty of Sciences, University of Novi Sad, under designation 2-0019.

2.3. Extract preparation

Pulverized and accurately weighted sample (3.1267 g) was extracted by maceration with 40 mL of cold methanol per cycle (4 cycles), with constant shaking. The pooled extract was filtered, and evaporated to dryness at 35 °C under reduced pressure. The obtained extract (88.3 mg) was stored in the dark at 4 °C until the HPLC analysis. The sample was dissolved in 1500 μL of methanol immediately before analysis.

2.4. LC-DAD-MS-MS analysis

Scan analysis was performed by liquid chromatography coupled with UV/Vis detection and tandem mass spectrometric detection. HPLC used was an Agilent Technologies 1200 Series Rapid Resolution system, consisting of a vacuum degasser, a binary pump, an autosampler, a thermostat, a column and a detector. It was coupled with a QqQ MS-MS detector with an electrospray (ESI) ion source. Instrument control and data acquisition was performed using MassHunter Workstation Data Acquisition v. B.01.02 software (Agilent Technologies). The sample (5 μL) was injected onto a Zorbax XDB-C18 50 mm × 4.6 mm × 1.8 μm column, thermostated at 50 °C. A gradient of 0.05% HCOOH and methanol (0 min 30% MeOH, 6 min 70%, 9 min 100%, 12 min 100%) was used as the mobile phase,

with a flow rate of 1 mL/min. The UV signals at 215 nm, 260 nm, 290 nm and 340 nm were monitored, as well as the continuous spectrum in the range 190–700 nm. Ion source parameters were: nebulization gas pressure of 50 psi, drying gas temperature of 350 °C, flow of 10 L/min, capillary voltage of 4000 V, fragmentor voltage of 135 V, positive- and negative-ionization mode. Compounds were monitored in MS2Scan mode, with *m/z* range of 100–1680.

To obtain additional structural information MS^n experiments were performed using Product Ion Scan mode, with $[M+H]^+$ or $[M+NH_4]^+$ as precursor ions, and collision energy of 10–40 V. High purity N_2 was used as collision gas. The results were processed using MassHunter Workstation Data Acquisition v. B.06.00 software (Agilent Technologies).

2.5. Compounds characterization

4'-*O*-demethylmorelensin (ASF354A, tentative identification): UV (MeOH) λ_{max} ~203sh, 234, 280 nm; $ESIMS^2$ (*m/z* 372 PI, 10 V) *m/z* 231 (100), 187 (10), 173 (1), 157 (5), 129 (2); $ESIMS^2$ (*m/z* 372 PI, 30 V) *m/z* 231 (7), 187 (34), 185 (21), 173 (40), 157 (62), 129 (100).

Kaerophyllin (ASF368A): $ESIMS^2$ (*m/z* 369 PI, 10 V) *m/z* 351 (51), 333 (7), 320 (32), 231 (15), 203 (49), 191 (11), 151 (10), 135 (100); $ESIMS^2$ (*m/z* 369 PI, 30 V) *m/z* 191 (16), 185 (18), 163 (18), 161 (10), 160 (16), 151 (41), 135 (100), 131 (10).

Isokaerophyllin (ASF368B): $ESIMS^2$ (*m/z* 369 PI, 10 V) *m/z* 351 (37), 333 (13), 320 (33), 231 (12), 217 (22), 216 (23), 203 (40), 150 (15), 135 (100); $ESIMS^2$ (*m/z* 369 PI, 30 V) *m/z* 319 (19), 302 (10), 191 (15), 173 (11), 163 (14), 161 (10), 160 (16), 151 (45), 135 (100).

Bursehernin (ASF370A): $ESIMS^2$ (*m/z* 369 PI, 10 V) *m/z* 353 (29), 335 (20), 161 (18), 151 (100), 135 (13), 131 (7); $ESIMS^2$ (*m/z* 369 PI, 30 V) *m/z* 151 (100), 135 (14), 131 (19), 103 (4).

4'-*O*-demethyldeoxypicropodophyllotoxin (ASF384A, tentative identification): UV (MeOH) λ_{max} 290, sh241, sh202 nm; $ESIMS^2$ (*m/z* 402 PI, 10 V) *m/z* 231 (100), 187 (26); $ESIMS^2$ (*m/z* 402 PI, 30 V) *m/z* 187 (72), 157 (85), 131 (4), 129 (100).

4'-*O*-demethyldeoxypodophyllotoxin (ASF384B, tentative identification): $ESIMS^2$ (*m/z* 402 PI, 10 V) *m/z* 231 (100), 187 (6); $ESIMS^2$ (*m/z* 402 PI, 30 V) *m/z* 231 (20), 213 (8), 187 (52), 185 (24), 173 (43), 157 (84), 129 (100).

Deoxypicropodophyllotoxin (ASF398A): $ESIMS^2$ (*m/z* 399 PI, 10 V) *m/z* 231 (100), 187 (69), 157 (14), 129 (6); $ESIMS^2$ (*m/z* 399 PI, 30 V) *m/z* 187 (30), 157 (51), 129 (100), 128 (5).

Deoxypodophyllotoxin (ASF398B): UV (MeOH) λ_{max} 291 nm; $ESIMS^2$ (*m/z* 399 PI, 10 V) *m/z* 231 (100), 187 (20), 173 (4), 157 (7); $ESIMS^2$ (*m/z* 399 PI, 30 V) *m/z* 231 (5), 213 (5), 187 (24), 185 (21), 173 (33), 157 (49), 129 (100), 128 (5).

Nemerosin (ASF398C): UV (MeOH) λ_{max} 315, 295, 238 nm; $ESIMS^2$ (*m/z* 399 PI, 10 V) *m/z* 363 (21), 353 (18), 350 (93), 231 (87), 221 (35), 213 (19), 203 (67), 187 (35), 181 (21), 157 (15), 135 (100); $ESIMS^2$ (*m/z* 399 PI, 30 V) *m/z* 221 (11), 203 (10), 191 (11), 190 (10), 185 (21), 181 (18), 173 (12), 166 (31), 161 (10), 160 (14), 157 (13), 135 (100), 129 (31).

Isochaihulactone (ASF398D): ESIMS^2 (*m/z* 399 PI, 10 V) *m/z* 363 (20), 353 (13), 350 (95), 349 (15), 231 (95), 221 (31), 213 (17), 203 (62), 187 (31), 181 (26), 157 (17), 135 (100); ESIMS^2 (*m/z* 399 PI, 30 V) *m/z* 350 (38), 349 (16), 348 (13), 335 (34), 333 (11), 307 (12), 305 (17), 221 (11), 191 (13), 190 (10), 185 (14), 181 (19), 173 (13), 166 (27), 160 (16), 157 (11), 135 (100), 129 (27).

Yatein (ASF400A): UV (MeOH) λ_{max} 286, 235, 200 nm; ESIMS^2 (*m/z* 401 PI, 10 V) *m/z* 383 (100), 365 (8), 223 (8), 181 (57), 161 (17), 135 (9), 131 (7); ESIMS^2 (*m/z* 401 PI, 30 V) *m/z* 181 (100), 166 (8), 161 (9), 148 (8), 135 (25), 131 (39), 103 (6).

Picropodophyllotoxin (ASF414A): ESIMS^2 (*m/z* 415 PI, 10 V) *m/z* 313 (10), 246 (12), 229 (36), 185 (100), 169 (15); ESIMS^2 (*m/z* 415 PI, 30 V) *m/z* 185 (100).

Podophyllotoxin (ASF414C): UV (MeOH) λ_{max} 216 nm; ESIMS^2 (*m/z* 415 PI, 10 V) *m/z* 397 (63), 379 (5), 351 (5), 312 (11), 247 (100), 229 (36), 219 (6), 203 (9), 185 (5), 144 (8); ESIMS^2 (*m/z* 415 PI, 30 V) *m/z* 282 (61), 228 (13), 202 (12), 200 (21), 184 (45), 172 (20), 145 (100), 135 (39), 126 (17), 117 (66).

7-*O*-hexosylpodophyllotoxin (ASF576A, tentative identification): UV (MeOH) λ_{max} 286, sh239, 202 nm; ESIMS^2 (*m/z* 594 PI, 10 V) *m/z* 397 (100), 313 (12); ESIMS^2 (*m/z* 594 PI, 30 V) *m/z* 397 (6), 313 (100), 298 (5), 282 (38), 229 (5).

7-*O*-coniferylpodophyllotoxin (ASF576B, tentative identification): UV (MeOH) λ_{max} sh314, sh295, 277, sh231, 206 nm; ESIMS^2 (*m/z* 594 PI, 10 V) *m/z* 397 (100), 229 (14); ESIMS^2 (*m/z* 594 PI, 30 V) *m/z* 397 (100), 379 (18), 351 (11), 312 (37), 298 (10), 282 (13), 229 (67), 185 (16).

3. RESULTS AND DISCUSSION

Most UV-active compounds unrelated to pigments eluted in the interval of moderate hydrophobicity, at 3.5–7 min (Fig. 1), where lignans were also expected to elute. For all detected peaks in this interval, with positive- and negative-ion MS^1 and UV spectra possibly corresponding to lignan structures, positive-ion MS^2 spectra were recorded. Additionally, since podophyllotoxin derivatives were detected in the preliminary tests, a systematic screening using the Precursor Ion Scan method was also applied, using $[PT+H–H_2O]^+$ ion at *m/z* 397 as targeted product. All the peaks were preliminarily labeled as ASF*xxxy*, where *xxx* is the molecular weight of the compound and *y* is an unique identifier, necessitated by the common occurrence of isobars. Structure elucidation was performed by the interpretation of mass and UV spectra (Orčić et al., 2021) and by automatic search of the internal library of lignans' mass spectra. This way, 15 lignans were identified, of which 13 were previously reported, and 2 were never before found in any biological source (Fig. 2).

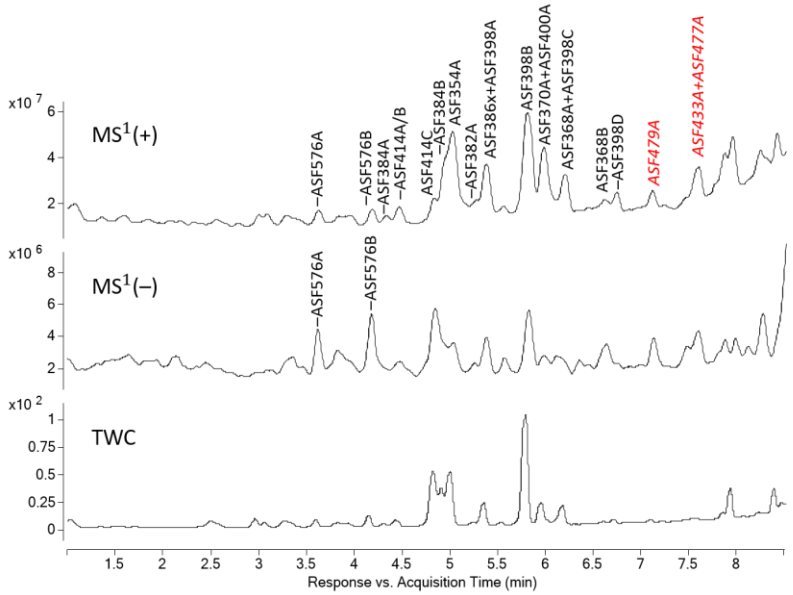

Fig. 1 Positive- and negative-ion mass chromatograms and total wavelength chromatogram of *A. sylvestris* fruit extract.

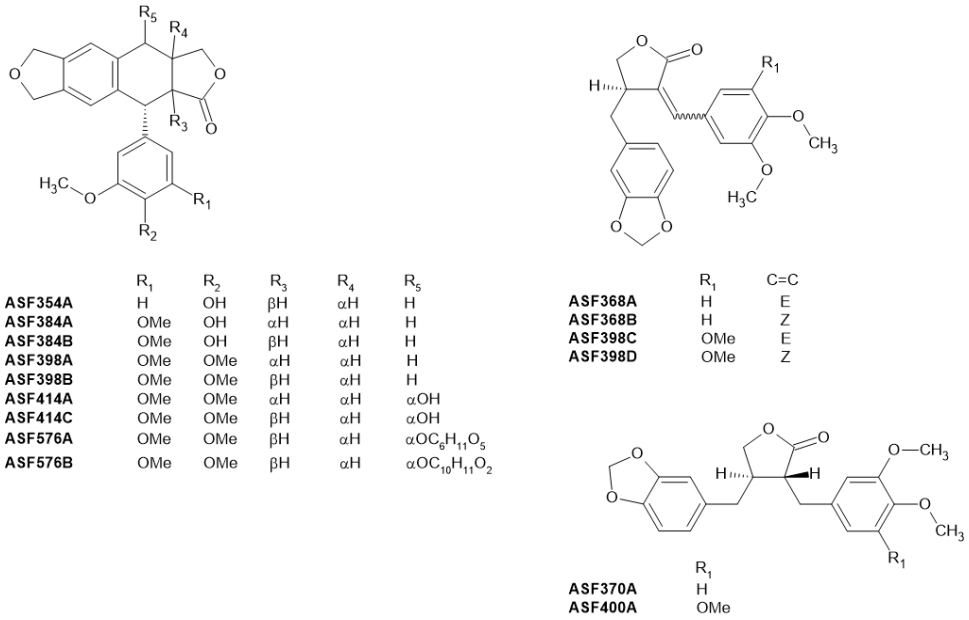

	R_1	R_2	R_3	R_4	R_5
ASF354A	H	OH	βH	αH	H
ASF384A	OMe	OH	αH	αH	H
ASF384B	OMe	OH	βH	αH	H
ASF398A	OMe	OMe	αH	αH	H
ASF398B	OMe	OMe	βH	αH	H
ASF414A	OMe	OMe	αH	αH	αOH
ASF414C	OMe	OMe	βH	αH	αOH
ASF576A	OMe	OMe	βH	αH	$\alpha OC_6H_{11}O_5$
ASF576B	OMe	OMe	βH	αH	$\alpha OC_{10}H_{11}O_2$

	R_1	C=C
ASF368A	H	E
ASF368B	H	Z
ASF398C	OMe	E
ASF398D	OMe	Z

	R_1
ASF370A	H
ASF400A	OMe

Fig. 2 Structures of the identified lignans.

3.1. Compound ASF354A

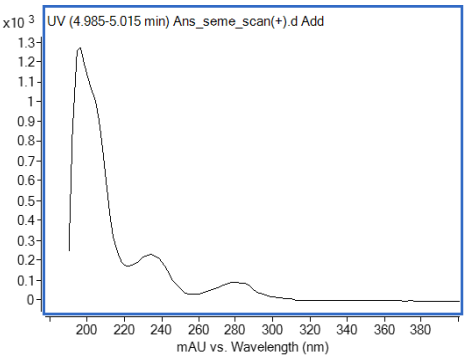

Fig. 3 UV spectrum of ASF354A.

The UV spectrum of compound ASF354A, with maxima at 280 nm, 234 nm and a shoulder at ~203 nm (Fig. 3), clearly indicated the absence of extended delocalization. Positive-ion MS^2 spectrum at low collision energy (V_{col} = 10 V) featured $[Cd+H]^+$ fragment the base peak (Fig. 4), which is characteristic of unsubstituted aryltetralins. The molecular weight of the $[Cd+H]^+$ fragment (*m/z* 231) corresponded to the methylenedioxy substitution. Based on the difference in molecular weights of $[M+H]^+$ and $[Cd+H]^+$ fragments, the molecular weight of the proximal phenyl was calculated to be 124, corresponding to the methoxy-hydroxy substitution. Negative-ionization MS^1 spectrum exhibited $[M–H]^–$ fragment, confirming the presence of phenolic hydroxyl. Therefore, the compound ASF354A was tentatively identified as 4'-hydroxy-3'-methoxy-4,5-methylenedioxy-2,7'-cyclolignano-9',9-lactone i.e. 4'-*O*-demethylmorelensin (Fig. 5). Unlike the majority of *A. sylvestris* lignans, which interact with tubulin and disrupt the microtubule-dependents processes including mitosis, 4'-*O*-demethyl derivatives can interact with the topoisomerase IIα-DNA complex and thus block the cell cycle in the late S or early G2 phase (Botta et al, 2001). Compound ASF354A has not been found in nature before.

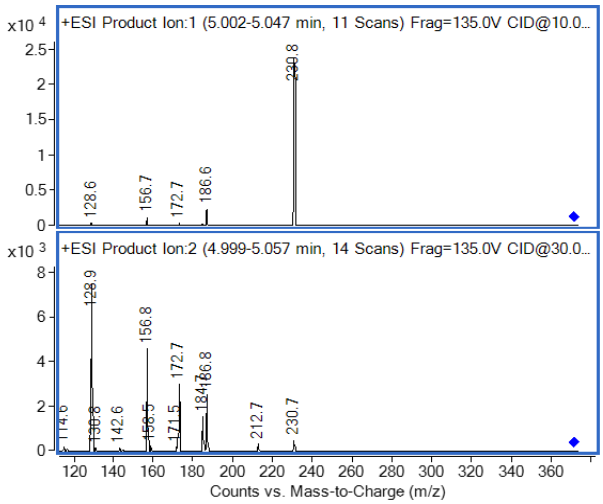

Fig. 4 Positive-ionization ESI-MS^2 spectra of ASF354A (V_{col} = 10 V and V_{col} = 30 V).

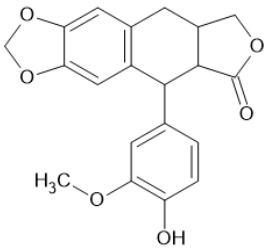

Fig. 5 Proposed structure of ASF354A.

3.2. Compounds ASF368A and ASF368B

Due to coelution, it was not possible to extract UV spectra of ASF368A and ASF368B. MS^2 spectra (Fig. S1 and Fig. S3) were nearly indistinguishable, indicating isomers. Positive-ion MS^2 spectra at V_{col} = 10 V was typical for unsaturated dibenzylbutyrolactones, characterized by moderate $[M+H–H_2O]^+$ (*m/z* 351) and $[M+H–2H_2O]^+$ (*m/z* 333) ions, weaker $[Cd+H]^+$ ion (*m/z* 231) accompanied by CO loss (*m/z* 203), as well as $[A]^+$ ions (*m/z* 135 as the base peak, and intense *m/z* 151). The molecular weights of $[Cd+H]^+$, $[Ad]^+$ and $[Ap]^+$ ions indicated methylenedioxy substitution on the distal ring and dimethoxy substitution on the proximal one. The spectra (Fig. S1 and Fig. S3) were in agreement with the library spectra of kaerophyllin (*E*-isomer) (Fig. S2) and isokaerophyllin (*Z*-isomer) (Fig. S4). Both compounds were already found in *A. sylvestris* (Orčić et al., 2021).

3.3. Compound ASF370A

Due to coelution, the UV spectrum of ASF370A could not be extracted. MS^2 spectra (Fig. S5) exhibited dominant $[A]^+$ ion (*m/z* 151), moderate $[M+H–H_2O]^+$ (*m/z* 353) and $[M+H–2H_2O]^+$ (*m/z* 335) ions, as well as minor $[A]^+$ (*m/z* 135) and $[B]^+$ (*m/z* 161) ions. The molecular weight of the $[Ap]^+$ ion (*m/z* 151) corresponded to a dimethoxy substitution on the proximal ring, while that of $[Ad]^+$ and $[Bd]^+$ suggested methylenedioxy substitution on the distal ring. The spectra (Fig. S5) were in agreement with the library spectra of bursehernin (Fig. S6), which was already found in *A. sylvestris* (Orčić et al., 2021).

3.4. Compound ASF384A and ASF384B

The UV spectrum of ASF384A (Fig. S7), with peak at 290 nm and shoulders at 241 nm and 202 nm, indicated a saturated structure, while the spectrum of ASF384B could not be extracted due to overlapping. MS^2 spectra were nearly indistinguishable (Fig. S8 and Fig. S10), indicating isomers. Positive-ion MS^2 spectra at low collision energy, typical for unsaturated aryltetralines, were characterized by $[Cd+H]^+$ fragment (*m/z* 231) as the base peak. MS^2 spectra exhibited $[Cd+H–CO_2]^+$ (*m/z* 187), $[Cd+H–CO_2–CH_2CO]^+$ (*m/z* 157) and $[Cd+H–CO_2–CH_2CO–CO]^+$ (*m/z* 129), which also appeared in the spectra of deoxypodophyllotoxin (Orčić et al., 2021). Together with the absence of $[Cd+H–CO]^+$ (*m/z* 203), characteristic of unsaturated dibenzylbutyrolactones, 7-hydroxyaryltetralins and 7-hydroxydibenzylbutyrolactones, this implied that the compounds ASF384A and ASF384B are aryltetralins with methylenedioxy substitution on the distal ring. Based on the difference in molecular weights of $[M+H]^+$ and $[Cd+H]^+$ fragments (154 units),

substitution on the proximal ring was identified as dimethoxy-hydroxy. Negative-ion MS spectra featured a weak $[M–H]^-$ ion, confirming the presence of phenolic hydroxyl group.

The only significant difference between the two isomers was observed in the positive-ion MS^2 spectra at V_{col} = 30 V – only spectra of ASF384B were characterized by $[Cd+H–CH_2CO]^+$ fragment (*m/z* 173) (Fig. S10). The configuration was determined by comparison with the spectra of deoxypodophyllotoxin and deoxypicropodophyllotoxin (ASF398A and ASF398B), identifying ASF384B and ASF384A as 4'-*O*-demethyldeoxypodophyllotoxin (Fig. S11) and 4'-*O*-demethyldeoxypicro podophyllotoxin (Fig. S9), respectively.

3.5. Compounds ASF398A-ASF398D

Mass spectra of compounds ASF398A and ASF398B (Fig. S12 and Fig. S15) clearly indicated unsubstituted aryltetralin structures. Positive-ion MS^2 spectra at V_{col} = 10 V were characterized by $[Cd+H]^+$ fragment (*m/z* 231) as the base peak, accompanied by $[Cd+H–CO_2]^+$ (*m/z* 187), $[Cd+H–CO_2–CH_2CO]^+$ (*m/z* 157) and $[Cd+H–CO_2–CH_2CO–CO]^+$ (*m/z* 129) fragments, which confirmed methylenedioxy substitution on distal ring. Based on difference in molecular weights of $[M+H]^+$ and $[Cd+H]^+$ fragments (168 units), substitution on the proximal ring was found to be trimethoxy. The UV spectrum of ASF398B (Fig. S14), with peak at 291 nm, confirmed unsubstituted aryltetralin structure. More abundant of the two isomers, ASF398B, was identified based on comparison of retention time and mass spectra with a standard as deoxypodophyllotoxin (Fig. S16) (Orčić et al., 2021). The spectra of this compound (Fig. S15), unlike of ASF398A (Fig. S12), featured $[Cd+H–CH_2CO]^+$ (*m/z* 173) fragment. Positive-ion MS^2 spectrum of the compound ASF398A at 10 V was characterized by prominent $[Cd+H–CO_2]^+$ (*m/z* 187) fragment, close to the base peak (Fig. S12). This compound was earlier identified as deoxypicropodophyllotoxin (Fig. S13) using alkaline isomerization (Orčić, 2010).

The mass spectra of the other two compounds (Fig. S18 and Fig. S20), ASF398C and ASF398D, were typical for unsaturated dibenzylbutyrolactones. The UV spectrum of ASF398C (Fig. S17) was characterized by peaks at 315 nm, 295 nm and 238 nm, indicating extended delocalization due to the presence of the cinnamate skeleton. MS^2 spectra of both compounds were characterized by $[Ad]^+$ (*m/z* 135) and $[Cd+H]^+$ (*m/z* 231) ions (Fig. S18 and Fig. S20). Molecular weights of both ions indicated methylenedioxy substitution of the distal ring, while the difference of molecular weights of $[M+H]^+$ and $[Cd+H]^+$ fragments (168 units) corresponded to trimethoxy substitution on the proximal ring. It follows that they are stereoisomeric (*E*)- and (*Z*)-3',4'-methylenedioxy-3,4,5-trimethoxylign-7-eno-9,9'-lactones, respectively nemerosin (Fig. S19) and isochaihulactone (Fig. S21), previously identified in *A. sylvestris* (Orčić et al., 2021). The stereochemistry of the isomers was determined based on the elution order.

3.6. Compound ASF400A

UV spectrum of ASF400A was characterized by maxima at 286 nm, 235 nm and 200 nm, what indicated the absence of extended delocalization (Fig. S22). MS^2 spectra had a profile characteristic for saturated dibenzylbutyrolactones (Fig. S23), with abundant $[M+H–H_2O]^+$ (*m/z* 383) and $[Ap]^+$ (*m/z* 181) fragments, and minor $[Bd]^+$ (*m/z* 161) and $[Ad]^+$ (*m/z* 135) fragments, which indicated methylenedioxy substitution on the distal ring and trimethoxy substitution on the proximal one. The identity of compound

ASF400A was confirmed by comparison with library spectra as yatein (Fig. S24), one of the most abundant lignans in *A. sylvestris* (Orčić et al., 2021).

3.7. Compounds ASF414C and ASF414A

Positive-ion MS^2 spectrum at V_{col} = 10 V (Fig. S27) was characterized by abundant $[M+H–H_2O]^+$ fragment at *m/z* 397, and by the pendant loss products from the intact and dehydrated ions, $[Cd+H]^+$ and $[Cd+H–H_2O]^+$ (*m/z* 247 and 229, respectively), but also by $[D+H]^+$ at *m/z* 313. MS^2 spectra were in agreement with literature (especially at V_{col} = 30 V), therefore compound ASF414C was identified as podophyllotoxin (Fig. S28), one of the previously found lignans in *A. sylvestris* (Orčić et al., 2021).

Another isomer, ASF414A, was characterized by a significantly different MS^2 spectra (Fig. S25) – minor $[D+H]^+$, $[Cd+H]^+$ and $[Cd+H–H_2O]^+$ ions at *m/z* 313, 247 and 229, and dominant $[Cd+H–H_2O–CO_2]^+$ ion at *m/z* 185. Compound ASF414A was identified as picropodophyllotoxin, previously reported in *A. sylvestris* (Orčić et al., 2021), by comparison of the spectrum with the library data (Fig. S26).

3.9. Compounds ASF576A and ASF576B

Compounds ASF576A and ASF576B were eluted at 3.6 min and 4.2 min. MS^1, and especially MS^2 spectra (Fig. S30 and Fig. 7) exhibited abundant $[PT+H–H_2O]^+$ ion at *m/z* 397, which is characteristic of podophyllotoxin and derivatives. MS^2 spectra (Fig. S30 and Fig. 7) were characterized by additional fragments – $[D+H]^+$ (*m/z* 313) and $[D+H–H_2O–CH_3O]^{\bullet+}$ (*m/z* 282), which confirmed podophyllotoxin core. Difference in molecular weights between $[M+H]^+$ and $[PT+H–H_2O]^+$ (180 units) commonly correspond to a hexose, caffeic acid or coumaryl alcohol.

Compound ASF576A eluted at a significantly shorter retention time than podophyllotoxin, indicating greater hydrophilicity. The UV spectrum (Fig. S29), with maxima at 286 nm, 239 nm (shoulder) and 202 nm, was practically identical to that of podophyllotoxin, indicating the absence of other UV active groups. Therefore, ASF576A was tentatively identified as 7-*O*-hexosylpodophyllotoxin (Fig. S31). Podophyllotoxin glucoside has previously been found in other plants, including *Podophyllum* (Broomhead and Dewick, 1990), but not in *A. sylvestris*.

The UV spectrum of compound ASF576B, with maxima at 314 nm (shoulder), 295 nm (shoulder), 277 nm, 231 nm (shoulder) and 206 nm, indicated extended delocalization and, therefore, ruling out the presence of a hexose (Fig. 6). By manual summation of experimental spectra of podophyllotoxin and coniferol derivatives (Fig. S32), the compound ASF576B was tentatively identified as 7-*O*-coniferylpodophyllotoxin (Fig. 8), which has never before been reported in nature.

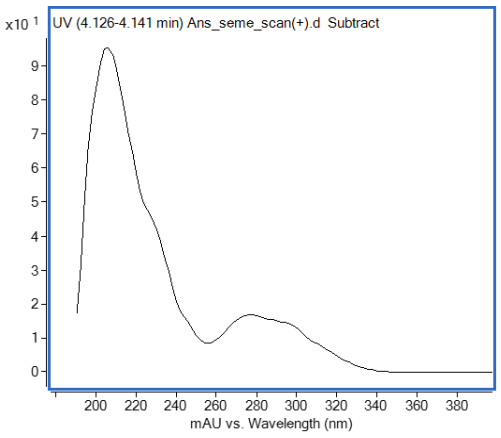

Fig. 6 UV spectrum of ASF576B.

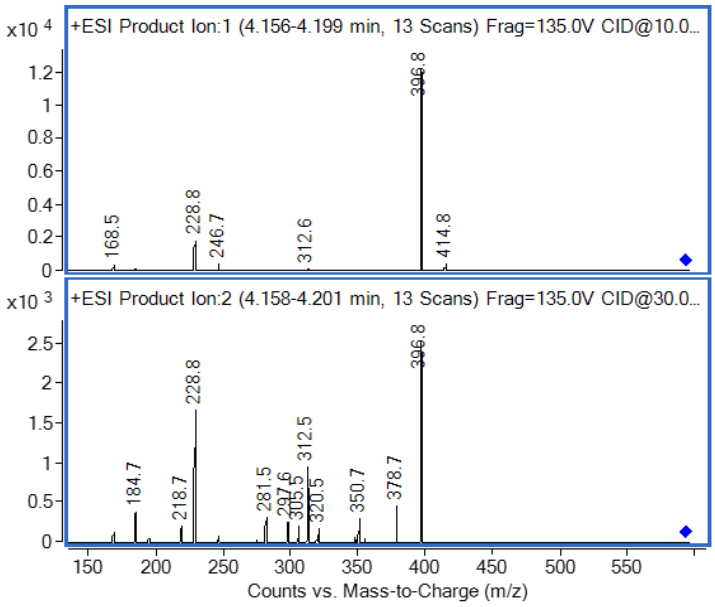

Fig. 7 Positive-ionization ESI-MS^2 spectra of ASF576B (V_{col} = 10 V and V_{col} = 30 V).

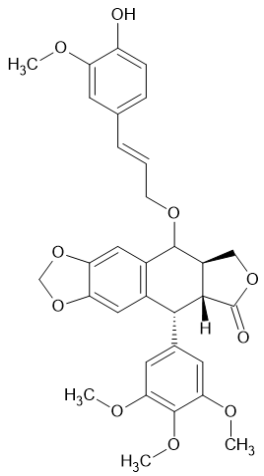

Fig. 8 Proposed structure of ASF576B.

To conclude, by LC-DAD-MS and LC-DAD-MS/MS analyses of *Anthriscus sylvestis* fruit extract, 15 lignans were detected and tentatively identified, of which 13 were previously found in *A. sylvestris*, and 2 were never reported in any biological source.

Acknowledgement: *The paper is a part of the research done within the project Grant Number 451-03-47/2023–01/200125. The authors would like to thank to the Ministry of Education, Science and Technological Development of the Republic of Serbia for the support of this research work.*

REFERENCES

Botta, B., Monache, G., Misiti, D., Vitali, A., Zappia, G., 2001. Curr. Med. Chem. 8(11), 1363-1381. doi: 10.2174/0929867013372292

Broomhead, A. J., Dewick, P. M., 1990. Phytochem. 29(12), 3831-3837. doi: 10.1016/0031-9422(90)85342-D

Chen, H., Jiang, H. Z., Li, Y. C., Wei, G. Q., Geng, Y., Ma, C. Y., 2014. Asian Pac. J. Cancer Prev. 15(6), 2803-2807. doi: 10.7314/APJCP.2014.15.6.2803

Chupakhina, G. N., Maslennikov, P. V., 2004. Russ. J. Ecol. 35, 290-295. doi: 10.1023/B:RUSE.0000040681.75339.59

Dall'Acqua, S., Giorgetti, M., Cervellati, R., Innocenti, G., 2006. Z. Naturforsch. C 61(9-10), 658-662. doi: 10.1515/znc-2006-9-1008

Hendrawati, O., Woerdenbag, H. J., Michiels, P. J., Aantjes, H. G., van Dam, A., Kayser, O., 2011. Phytochem. 72(17), 2172-2179. doi: 10.1016/j.phytochem.2011.08.009

Ikeda, R., Nagao, T., Okabe, H., Nakano, Y., Matsunaga, H., Katano, M., Mori, M., 1998. Chem. Pharm. Bull. 46(5), 875-878. doi: 10.1248/cpb.46.875

Kozawa, M., Baba, K., Matsuyama, Y., Kido, T., Sakai, M., Takemoto, T., 1982. Chem. Pharm. Bull. 30(8), 2885-2888. doi: 10.1248/cpb.30.2885

Lin, C. X., Son, M. J., Ju, H. K., Moon, T. C., Lee, E., Kim, S. H., Kim, M. J., Son, J. K., Lee, S. H., Chang, H. W., 2004. Planta Med. 70(05), 474-476. doi: 10.1055/s-2004-818981

Miller, T. W., D'Auria, D. E., 2011. Invasive Plant Sci. Manag. 4(3), 326-331. doi: 10.1614/ipsm-d-10-00068.1

Milovanovic, M., Stefanovic, M., Djermanovic, V., Milovanovic, J., 1996. J. Herbs Spices Med. Plants. 4(2), 17–22. doi: 10.1300/j044v04n02_04

Olaru, O. T., Niţulescu, G. M., Orţan, A., Băbeanu, N., Popa, O., Ionescu, D., Dinu-Pirvu, C. E., 2016. Rom. Biotechnol. Lett. 22(6), 12054. doi: 10.3390/molecules200815003

Orčić, D., 2010. Doctoral dissertation, University of Novi Sad (Serbia).

Orčić, D., Berežni, S., Škorić, D., Mimica-Dukić, N., 2021. Phytochem. 192, 112958. doi: 10.1016/j.phytochem.2021.112958

Orčić, D., Berežni, S., Mimica-Dukić, N., 2022a. Molecules 27(18), 6072. doi: 10.3390/molecules27186072

Orčić, D., Berežni, S., Mimica-Dukić, N., 2022b. Biol. Serb. 44(1), 41-51. doi: 10.5281/zenodo.7074977

PROFIL LIGNANA IZ PLODA ŠUMSKE KRASULJICE (*ANTHRISCUS SYLVESTRIS* (L.) HOFFM.)

Šumska krasuljica (Anthriscus sylvestris), poznata i kao velika krasuljica ili velika krbuljica, jeste široko rasprostranjena zeljasta biljna vrsta iz familije Apiaceae. Tradicionalna upotreba kao analgetik, antipiretik, antitusik, tonik, diuretik i dr. povezana je sa dokazanim prisustvom različitih klasa biomolekula, pre svega lignana koji poseduju citotoksičnost, antiproliferativnu, insekticidnu, antiviralnu i druge aktivnosti. Najveći broj jedinjenja pripada dvema klasama lignana – ariltetralinima i dibenzilbutirolaktonima. Podaci o profilu lignana iz A. sylvestris su uglavnom ograničeni na sastav korena i herbe, stoga je LC-DAD-ESI-MS/MS tehnika korišćena za identifikaciju 15 jedinjenja iz ekstrakta ploda A. sylvestris, od kojih dva nikada pre nisu nađena u prirodi.

Ključne reči: *Anthriscus sylvestris, Apiaceae, ESI-MS, HPLC, lignan, određivanje strukture.*